

Correlated transport of FQHE quasiparticles in a double-antidot system

Dmitri V. Averin and James A. Nesteroff

Department of Physics and Astronomy, Stony Brook University, SUNY, Stony Brook, NY 11794-3800

Abstract

We have calculated the linear conductance associated with tunneling of individual quasiparticles of primary quantum Hall liquids with filling factors $\nu = 1/(2m + 1)$ through a system of two antidots in series. On-site Coulomb interaction simulates the Fermi exclusion and makes the quasiparticle dynamics similar to that of tunneling electrons. The liquid edges serve as the quasiparticle reservoirs, and also create the dissipation mechanism for tunneling between the antidots. In the regime of strong dissipation, the conductance should exhibit resonant peaks of unusual form and a width proportional to the quasiparticle interaction energy U . In the weakly-damped regime, the shape of the resonant conductance peaks reflects coherent tunnel coupling of the antidots. The Luttinger-liquid singularity in the rates of quasiparticle tunneling to/from the liquid edges manifests itself as an additional weak resonant structure in the conductance curves.

Key words: Fractional Quantum Hall Effect; Quasiparticle tunnelling; Quantum Computation

PACS: 73.43.-f, 05.30.Pr, 71.10.Pm, 03.67.Hk

1. Introduction

Quasiparticles of two-dimensional (2D) electron liquids in the regime of the Fractional Quantum Hall effect (FQHE) have the unusual properties of fractional charge [1] and fractional exchange statistics [2,3]. Quantum antidots formed in the 2D electron system offer a possibility of localizing and controlling transport of individual quasiparticles [4,5,6]. Such a control made possible the first direct observation of the fractional quasiparticle charge in tunneling through an antidot [4]. This observation was later extended to the regime of ballistic quasiparticle transport [7,8].

The mechanism of quasiparticle localization on antidots relies on the combined action of the electric and magnetic field and is microscopically quite different from the corresponding features of electron localization in quantum dots. Nevertheless, transport phenomena in antidots are very similar to those associated with the Coulomb blockade in tunneling of individual electrons [9]. For instance, in close analogy to the Coulomb-blockade oscillations of conductance of the quantum dots [10], the antidots exhibit periodic conductance oscillations with each period corresponding to addition of one quasiparticle to the antidot [4,5,6]. So far, antidot transport has been studied both experimentally [4,5,6] and theoretically [11] for one antidot. In this work, we develop a theory of correlated transport of individual quasiparticles through two antidots. The double-antidot system

was discussed previously [12] as a qubit, information in which is encoded by individual quasiparticles. Such qubit is similar to superconducting charge qubits [13,14] which are based on the dynamics of individual Cooper pairs. As in the case of Cooper pairs [15,16], the transport measurements on the quasiparticle qubit can be done more easily than direct measurements of the qubit dynamics. Transport measurements would constitute the first step towards experimental development of the FQHE qubits. More generally, understanding the transport properties of multi-antidot systems, in particular the role of Coulomb interaction for localization of individual quasiparticles, and significance of the edge-state decoherence, should also be important for other, more complicated types of suggested FQHE qubits [17,18] which also require control over individual quasiparticles.

2. Model

The system we consider consists of two antidots in series between the two opposite edges of a primary quantum Hall liquid with the filling factor $\nu = 1/(2m + 1)$ (Fig. 1a). The antidots are tunnel-coupled to each other and to the edges, which play the role of quasiparticle reservoirs. The quasiparticle current through the antidots is driven by the transport voltage V applied between the edges. The focus of this work is on the regime when all relevant energies are smaller than the energy gap Δ^* of the antidots (see below),

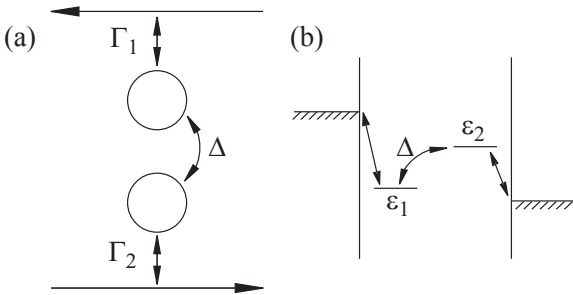


Fig. 1. Quasiparticle tunneling in the double-antidot system: (a) the real-space geometry (not to scale) of quasiparticle transfer between the opposite edges of the FQHE liquid; (b) energy diagram of the transfer.

and the transport can be described completely in terms of the transfer of individual quasiparticles. This regime is relevant, e.g., for the operation of this system as a qubit. The main elements of the model of the double-antidot system in this case can be outlined as follows.

2.1. Antidots

An antidot formed at a point ζ in a primary quantum Hall liquid with the filling factor $\nu = 1/(2m+1)$ can be described as a collection of n quasi-hole excitations created at this point. Microscopically, the unnormalized wavefunction of this configuration is [1]:

$$\psi(\{z_j\}) = \prod_j (z_j - \zeta)^n \psi_m(\{z_j\}), \quad (1)$$

where $\psi_m(\{z_j\})$ is the Laughlin's wavefunction of the unperturbed quantum Hall liquid and, in the standard notations, the antidot position ζ in the two-dimensional plane and the electron coordinates z_j are given in the complex form and normalized to the characteristic length $\ell = (\hbar/eB)^{1/2}$ in the magnetic field B . The number n of the quasiholes is related to the geometric radius R of the antidot: $R \simeq \sqrt{2n\ell}$.

In what follows, we make use only of the general qualitative features of the wavefunction (1). For instance, in agreement with the typical experimental situation (see, e.g., [4]), we assume that the antidot is relatively large: $n \gg 1$. This means that addition/removal of individual quasiparticles (here and below, this term will be used to describe processes with varying n : $n \rightarrow n \pm 1$), does not change the antidot parameters noticeably. Indeed, the variation of the antidot radius in this case is $\delta R \propto \ell/\sqrt{n}$ and is small not only on the scale of R , but, more importantly, on the scale of the magnetic length ℓ .

The general form of the antidot energy E_n as a function of n is determined by the interplay of Coulomb interaction and an external potential used to create the antidot. However, for large n , and in some small range of variation of n around the minimum of E_n , one can always approximate this dependence as quadratic. This defines the character-

istic energy gap $\Delta^* \equiv \partial^2 E_n / \partial n^2$ which gives the energy interval of variation of the chemical potential μ of the system between the successive additions of individual quasiparticles to the antidot. For the system shown in Fig. 1a, the antidots exchange quasiparticles with the edges, and μ is defined by the edge chemical potential. In the situation of the antidot, when all the energies are dominated by the Coulomb repulsion, the energy gap Δ^* for changing the number of quasiparticles is approximately related to the energy gap for the antidot excitations at fixed n : $\Delta^* \simeq \hbar u / 2\pi R$, where u is the velocity of the excitations encircling the antidot. In general, e.g. in the case of quantum dots, the two types of energy gaps can be very different.

We assume that the gap Δ^* is sufficiently large for both antidots of the double-antidot system, so that in the reasonably large range of variation of μ both antidots are characterized by some well-defined numbers n_l , $l = 1, 2$, of the quasiparticles. In this regime, the non-vanishing conductance of the double-antidot system requires that μ is close to resonances in the both antidotes. At resonance, $E_{n_l} \simeq E_{n_{l+1}}$, and each antidot can in principle be in one of two states which differ by the presence/absence of one "extra" quasiparticle. The resulting four double-antidot states are relevant for the quasiparticle transport. We will use the notation for these states that gives the number of extra quasiparticles on each antidot:

$$|ij\rangle \equiv |n_1 + i, n_2 + j\rangle, \quad i, j = 0, 1, \quad (2)$$

and talk about the "first" and the "second" quasiparticle on the antidots disregarding the background n_l quasiparticles. Counting the antidot energies E_n from the energy of the state with no extra quasiparticles, we can parameterize the energies ϵ_{ij} of the four states as

$$\epsilon_{00} = 0, \quad \epsilon_{11} = 2\epsilon + U, \quad \epsilon_{10} = \epsilon - \delta, \quad \epsilon_{01} = \epsilon + \delta. \quad (3)$$

Here U is the interaction energy between the extra quasiparticles on the two antidots, and ϵ and δ give the energies ϵ_l (Fig. 1b) of the single-quasiparticle states localized at the two antidots: $\epsilon_{1,2} = \epsilon \pm \delta$. The energies ϵ and δ are defined relative to the common chemical potential of the edges for vanishing bias voltage V between them. Non-vanishing bias voltage shifts the energies (3). Experimentally, the antidot energies are controlled by the back-gate voltage or magnetic field [4,5]. The degree to which these fields couple to the energy difference δ depends on the degree of asymmetry between the two antidots. In the following, we present the results for quasiparticle conductance of the system as a function of ϵ for fixed δ , as would be appropriate for identical antidots. These results can be generalized to non-identical antidots by taking a "cross-section" in the space of ϵ and δ along the direction appropriate for a given degree of the antidot asymmetry.

If the two antidots are sufficiently close, so that the distance between their edges is on the order of magnetic length ℓ , the quasiparticle states localized around them overlap and hybridize. This effect can be accounted for by the tunnel coupling $-\Delta$ of the antidots. The phases of the antidot

states can always be chosen to make Δ real. This coupling affects only the singly-occupied states $|10\rangle$ and $|01\rangle$. The single-quasiparticle part of the Hamiltonian is then:

$$H = \epsilon - \delta\sigma_z - \Delta\sigma_x, \quad (4)$$

where σ 's are the Pauli matrices. Equation (4), together with the part of Eq. (3) describing states with zero and two quasiparticles, give the main part of the antidot energy controlling the quasiparticle transport. In what follows, we assume that all contributions to this energy and the temperature T are small:

$$\Delta, \varepsilon_l, U, T \ll \Delta^*. \quad (5)$$

In this regime, tunneling through the antidots can be discussed in terms of correlated transfer of individual quasiparticles. Since the gap Δ^* is dominated by the Coulomb interaction, i.e. has the same origin as the quasiparticle interaction energy U , the most restrictive part of the assumption (5) is the condition on U . This condition can still be satisfied, due to the difference between stronger quasiparticle repulsion on the same site and weaker repulsion on different sites.

2.2. Antidot-edge tunneling

Similarly to the tunnel coupling between the antidots, if the edges of the FQHE liquid are not far from the antidots on the scale of the magnetic length ℓ , there is a non-vanishing amplitude for quasiparticle tunneling between the edge and the nearest antidot. The tunneling between the l th edge and antidot can be described quantitatively with the standard tunnel Hamiltonian

$$H_T^{(l)} = T_l \psi_l^\dagger \xi_l + h.c., \quad (6)$$

where ψ, ψ^\dagger and ξ, ξ^\dagger are the creation/annihilation operators for quasiparticles at, respectively, the edges and the antidots. Denoting the position along the edge as x and taking the tunneling points for both edges to be at $x = 0$, the edge quasiparticle operators ψ_l can be expressed in the standard bosonisation approach as [19]

$$\psi_l(t) = (1/2\pi\alpha)^{1/2} \tilde{\xi}_l e^{i\sqrt{\nu}\phi_l(0,t)}. \quad (7)$$

Here the “Klein factors” $\tilde{\xi}_l$ account for the mutual statistics of the quasiparticles in different edges, ϕ_l are the chiral bosonic fields which describe the edge fluctuations propagating with velocity u , and $1/\alpha$ is their momentum cut-off. The edge fluctuations result in the fluctuations of electron density at the edge: $\rho_l(x, t) = (\sqrt{\nu}/2\pi)\partial\phi_l(x, t)/\partial x$. Both fields ϕ_l can be decomposed in the standard way into the individual “magneto-plasmon” oscillator modes a_n, a_n^\dagger :

$$\phi(x, t) = \sum_{n=1}^{\infty} \frac{1}{\sqrt{n}} \left[a_n e^{iq_n(x+ia)} + h.c. \right], \quad q_n = 2\pi n/L, \quad (8)$$

where L is a normalization length. In the geometry of the double-antidot system, there are no interference loops for

the edge quasiparticle. In this case, the statistical Klein factors in (7) would cancel out in the perturbation expansion in tunneling (6) and can be omitted.

The quasiparticles at the antidots should be described in general by the expressions similar to Eq. (7). Condition (5) of the large antidot energy gap Δ^* ensures, however, that the fluctuations of the edges around the antidots are suppressed, i.e. the magneto-plasmon oscillations are not excited out of their ground state $|0\rangle$. In this regime of the “quantized” edge, the general quasiparticle operators (7) reduce to just the statistical Klein factors up to a normalization constant. Indeed, as one can see directly from Eq. (8) by bringing the ϕ -part of (7) into the normal form,

$$\langle 0 | e^{i\sqrt{\nu}\phi} | 0 \rangle / (2\pi\alpha)^{1/2} = (\pi R)^{-1/2}. \quad (9)$$

Including this normalization constant in the tunnel amplitude T_l , we see that the operators ξ_l for quasiparticles at the antidots consist solely of the Klein factors. The appropriate set of properties of the quasiparticle Klein factors ξ depends on the specific geometry of each edge-state tunneling problem. Non-trivial examples of this can be found in [20,21,22,23,24]. As follows from the discussion in the preceding Section, in tunneling between the quantum antidots, the operators ξ_l should account for the “hardcore” property of the quasiparticles: In the given range of external parameters only one extra quasiparticle can occupy one antidot. In general, these operators should also describe the anyonic exchange statistics of the FQHE quasiparticles, but the geometry of the double-antidot system (Fig. 1a) does not permit quasiparticle exchanges, and the exchange statistics of the tunneling particles is irrelevant. Since the hardcore property makes the quasiparticle occupation factors equivalent to those of the fermions, and the actual exchange statistics is irrelevant, the antidot quasiparticle operators ξ, ξ^\dagger can be treated as fermions. Together with Eqs. (7) and (8) for the edge quasiparticles, this defines completely the tunnel Hamiltonian (6).

2.3. Edge-state decoherence

Tunneling of charged quasiparticles through the antidot system couples to all gapless charged excitations that exist in the system. In the case of the FQHE liquid, excitations in the bulk of the liquid are suppressed by the energy gap, and only the edges support gapless excitations. In contrast to all other possible mechanisms of decoherence (e.g., plasmons in metallic gates, or charged impurities in the substrate) the edges play the role of reservoirs in transport measurements and as a matter of principle can not be removed from the antidots. In this Section, we estimate the strength of this unavoidable edge-state decoherence for quasiparticle tunneling through the double-antidot system.

The spectrum of the gapless edge excitations of one edge consists of magneto-plasmon oscillations (8) with the Hamiltonian:

$$H_0 = (hu/L) \sum_{n=1}^{\infty} n a_n^\dagger a_n. \quad (10)$$

We assume that the antidot system is symmetric, and a quasiparticle sitting on the first antidot creates a potential $V_l(x)$ along the l th edge. The quasiparticle dynamics governed by the Hamiltonian (4) is coupled then to the fluctuations of electron densities $\rho_l(x)$ at the edges through the interaction Hamiltonian

$$H_{int} = \frac{1}{2} \sigma_z e \int dx V(x) (\rho_1(x) - \rho_2(x)), \quad (11)$$

where $V(x) = V_1(x) - V_2(x)$ is the change of the potential along the edges due to quasiparticle transfer between the antidots. Since the edge-antidot distance and the distance between the antidots are on the order of antidot radius R , this radius sets the range of the potential $V(x)$. The edge velocity u can be expected to be similar for the external edges and the antidots. This means that the condition (5) of the large energy gap implies that the characteristic wavelength of the edge excitations which can exchange energy with the quasiparticles on the antidots is much larger than the range of the potential $V(x)$: $\hbar u/\epsilon \gg \hbar u/\Delta^* \simeq R$. The interaction energy (11) can be expressed then as

$$H_{int} = \frac{e}{2} \sigma_z (\rho_1(0) - \rho_2(0)) \int dx V(x), \quad (12)$$

where, as follows from Eq. (8), the densities ρ_l are

$$\rho_l(0) = \frac{i\sqrt{\nu}}{L} \sum_{n=1}^{\infty} \sqrt{n} (a_n - a_n^\dagger). \quad (13)$$

The strength of interaction (12) can be characterized by the typical transition rate Γ_d between the eigenstates of the antidot Hamiltonian (4) induced by the edges. Straightforward calculation of the “Golden-rule” rate using Eqs. (10), (12), and (13) gives:

$$\Gamma_d = \frac{\nu^3}{4\pi\hbar} \alpha^2 \kappa^2 |\langle \sigma_z \rangle|^2 \frac{\Delta E}{1 - e^{-\Delta E/T}}, \quad (14)$$

where ΔE is the energy difference between the two states, $\langle \sigma_z \rangle$ is the matrix element of σ_z between them. The dimensionless factor κ characterizes the overall “intensity” of the antidot-edge potential:

$$\kappa \equiv \left(\frac{\nu e}{4\pi\epsilon\epsilon_0} \right)^{-1} \int dx V(x), \quad (15)$$

The precise form of the potential $V(x)$ and the value of κ depend on the details of configuration of the metallic gates that define the edges and screen the antidot-edge interaction. However, normalized as in Eq. (15), κ should be on the order of 1. For instance, assuming as a crude model of the system electrostatics that the antidot-edge interaction is confined to the interval $d \simeq 2R$ in which the edge is a tunnel-limited distance ℓ away from the antidot, one can estimate κ as $(2/\pi) \ln(2R/\ell)$, i.e., $\kappa \simeq 2$ for realistic $R/\ell \simeq 10$.

The factor α in (14) is the “fine structure constant” of the edge excitations:

$$\alpha \equiv \frac{e^2}{4\pi\epsilon\epsilon_0\hbar u}, \quad (16)$$

and is the main parameter controlling the strength of decoherence Γ_d through the velocity u of the edge excitations. The dielectric constant ϵ is fixed by the material (GaAs) of the structure: $\epsilon \simeq 10$, and in the realistic range of possible velocities u , $10^4 \div 10^5$ m/s [5], α should vary in the range between 2 and 20. In the most relevant case of the FQHE liquid with the filling factor $\nu = 1/3$, and for the edge-antidot coupling intensity estimated above, the quality factor $\Delta E/\hbar\Gamma_d$ of the quasiparticle dynamics changes then roughly between 0.1 and 10. This means that in the case of strong edge confinement that produces large velocity u , the quasiparticle dynamics on the antidots can be quantum-coherent provided that all other decoherence mechanisms are sufficiently weak. In the opposite case of smooth confinement with low velocity u , the already unavoidable edge-state decoherence is strong enough to completely suppress the coherence of the quasiparticle states on different antidots, and quasiparticle transfer processes between them are incoherent.

3. Tunneling rates

As was mentioned above, the discussion in this work is limited to the regime in which the transport through the double-antidot system can be interpreted as the correlated transfer of individual quasiparticles. Besides the condition (5) on antidot energies, this also requires that the antidots are coupled only weakly to the edges, so that the edge-antidot tunneling can be treated as a perturbation leading to an incoherent transfer of individual quasiparticles. The quasiparticle transport through the antidots is governed then by the kinetic equation similar to that for Coulomb-blockade transport in quantum dots with discrete energy spectrum [25]. This Section calculates the relevant tunneling rates in the two limits of strong and weak edge-state decoherence.

3.1. Strong decoherence

If the edge-state decoherence is sufficiently strong, the quasiparticle transfer between the antidots can be treated as incoherent and described by the sequential tunneling rate obtained by perturbation theory in the tunnel amplitude Δ . To calculate this rate, it is convenient to express the density operators ρ_l of the two edges through one effective density ρ which satisfies the same relation (13): $\rho_1(0) - \rho_2(0) \rightarrow \sqrt{2}\rho(0)$, so that the edge-antidot coupling (12) is:

$$H_{int} = \hbar u \nu \frac{\kappa\alpha}{\sqrt{2}} \rho(0) \sigma_z. \quad (17)$$

Next, one can perform a unitary transformation which converts the fluctuations of the energy of the quasiparticle basis states $|10\rangle, |01\rangle$ induced by (17) into a fluctuating phase of the tunneling matrix elements of the tunneling part of the Hamiltonian (4):

$$-\Delta\sigma_x \rightarrow -\Delta \sum_{\pm} \sigma_{\pm} e^{\pm i\sqrt{g}\phi(0,t)}, \quad g = \frac{\nu^3 \kappa^2 \alpha^2}{2\pi^2}, \quad (18)$$

where $\phi(x,t)$ is the bosonic field given by same the Eq. (8). Then, the rate Γ_{Δ} of the *anidot-antidot* tunneling can be expressed in the lowest non-vanishing order in the amplitude Δ as:

$$\Gamma_{\Delta} = 2\Delta^2 \text{Re} \int_{-\infty}^0 dt e^{iEt} \langle e^{i\sqrt{g}\phi(0,t)} e^{-i\sqrt{g}\phi(0,0)} \rangle, \quad (19)$$

where $\langle \dots \rangle$ is the average over the equilibrium fluctuations of ϕ and $E = \pm 2\delta$ is the energy difference (depending on the direction of tunneling) between the quasiparticle states localized on the antidots. The standard evaluation of Eq. (19) (see, e.g., [26,27]) gives:

$$\Gamma_{\Delta}(E) = \gamma f_g(E), \quad \gamma \equiv 2\pi\Delta^2/\omega_c, \quad (20)$$

$$f_g(E) \equiv \frac{1}{2\pi\Gamma(g)} (2\pi T/\omega_c)^{g-1} |\Gamma(g/2 + iE/2\pi T)|^2 e^{-E/2T},$$

where $\Gamma(z)$ is the gamma-function and $\omega_c = \hbar u/2\alpha$ is the cut-off energy of the edge excitations. The function $f_g(E)$ gives the energy dependence of the tunneling rate (see Fig. 2) and is defined to coincide with the Fermi distribution function for $g = 1$. The power g determines the behavior of the transition rate at large energies $|E| \gg T$: $\Gamma_{\Delta}(E) \propto E^{(g-1)}$ on the “allowed” side of the transition ($E < 0$), and $\Gamma_{\Delta}(E) \propto E^{(g-1)} e^{-E/T}$ on the “forbidden” side ($E > 0$), when the transition has to overcome the energy barrier E . This asymptotic behavior of the tunneling rates, together with Eq. (20), is valid at $|E| \ll \omega_c$.

The rates Γ_l , $l = 1, 2$, of the *antidot-edge* tunneling are obtained through a similar calculation starting with the tunnel Hamiltonian (6). They are given by the same expression (20):

$$\Gamma_l(E) = \gamma_l f_{\nu}(E), \quad \gamma_l \equiv 2\pi|T_l|^2/\omega_c. \quad (21)$$

In general, the long-range Coulomb interaction should generate corrections to g which move it away from the “quantized” value $g = \nu$ [28]. However, in contrast to the quasiparticle tunneling between the antidots, which is changed qualitatively by decoherence created by the Coulomb interaction with the edge, the Coulomb corrections for the antidot-edge tunneling are expected to be small and will be neglected in this work.

Thus, in the regime of strong edge-state decoherence, the overall transport of quasiparticles through the double-antidot system can be described as a combination of successive antidot-edge transitions (21) and incoherent transitions (20) between the antidots.

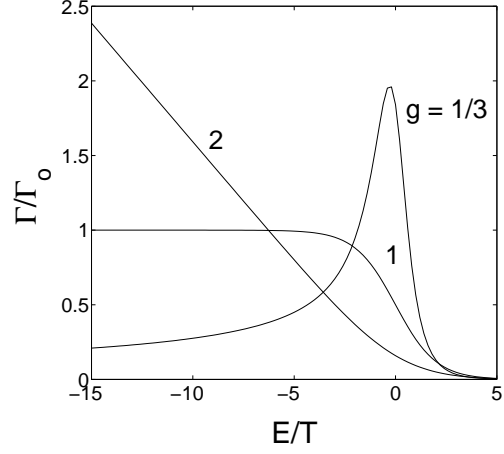


Fig. 2. Energy dependence of the antidot-antidot (20) and antidot-edge (21) tunneling rates. The normalization factor is $\Gamma_0 = \gamma(2\pi T/\omega_c)^{g-1}$.

3.2. Weak decoherence

For sufficiently strong edge-state confinement, the edge-induced relaxation rate (14) will be smaller than the antidot energies. If other decoherence mechanisms, including the decoherence created by incoherent antidot-edge tunneling are also weak on the scale of the antidot energies,

$$\Gamma_d, \Gamma_l \ll \Delta, \delta, U, T, \quad (22)$$

the quasiparticle dynamics on the antidots is quantum-coherent. It is characterized by the stationary eigenstates $|k\rangle$, $k = 1, 2$, of the double-antidot Hamiltonian (4):

$$H|k\rangle = (\epsilon + (-1)^k \Omega)|k\rangle, \quad \Omega \equiv (\delta^2 + \Delta^2)^{1/2},$$

$$|k\rangle = c_{1k}|10\rangle + c_{2k}|01\rangle, \quad (23)$$

for which the probabilities λ_{lk} of finding the quasiparticle on the l th antidot are:

$$\lambda_{lk} = |c_{lk}|^2 = [1 + (-1)^{l+k} \delta/\Omega]/2. \quad (24)$$

In the coherent regime (22), the double-antidot system can be viewed as a quasiparticle qubit [12]. The current through the qubit is described in terms of tunneling to/from the eigenstates (23). The corresponding tunneling rates are found from the tunnel Hamiltonian (6), in which, as was discussed in Sec. 2.2, the quasiparticle creation/annihilation operators ξ, ξ^{\dagger} act as fermions. This means that the tunnel matrix elements for the quasiparticles can be calculated in the standard way. In particular, for each eigenstate (23), the matrix element is independent of the occupation factor of the other eigenstate. Explicitly, the tunneling rate Γ_{lk} from the l th edge into the state $|k\rangle$ is

$$\Gamma_{lk} = 2|T_l|^2 |\langle k | \xi_l^{\dagger} | 0 \rangle|^2 \text{Re} \int_{-\infty}^0 dt e^{iEt} \langle \psi_l^{\dagger}(t) \psi_l(0) \rangle. \quad (25)$$

Here $|0\rangle$ denotes the empty eigenstate and E is the appropriate tunneling energy which includes in general the

eigenenergies (23) and the interaction energy U . The quasiparticle matrix elements are $|\langle k|\xi_l^\dagger|0\rangle|^2 = \lambda_{lk}$, and we get:

$$\Gamma_{lk}(E) = \lambda_{lk}\Gamma_l(E), \quad (26)$$

where the rates $\Gamma_l(E)$ are given by Eq. (21). In the practically important case of FQHE liquid with $\nu = 1/3$, the energy dependence of the transition rates (26) is illustrated by the $g = 1/3$ curve in Fig. 2. The peak of the tunneling rate at $\epsilon \simeq 0$ is the consequence of the Luttinger-liquid correlations of the edge quasiparticles. Conductance calculations presented in the next Section show that this peak manifests itself as additional resonant features of the qubit conductance.

4. Conductance of the double-antidot system

In both situations of strong and weak decoherence, the conductance associated with tunneling of individual quasiparticles through the double-antidot system can be calculated by solving the kinetic equation for quasiparticle occupation probabilities of the antidot states. Similarly to the case of tunneling through one antidot [4,5,6,11], the conductance as a function of the common energy ϵ of the antidot states should exhibit the resonant tunneling peaks. For the double-antidot system, the peak structure is, however, more complicated, reflecting the transition between the low-temperature regime in which each peak corresponds to addition of one quasiparticle to the system of antidots, and a possible “large-temperature” regime, when the single-quasiparticle peaks are merged, and each conductance peak is associated with addition of two quasiparticles. In this Section, we calculate the corresponding conductance line shapes. Quantitatively, these line shapes are determined by the interplay between the quasiparticle repulsion energy U on the two antidots and tunnel coupling Δ between them. The calculations below are focused mostly on the more typical case of large repulsion energy $U \gg \Delta \simeq \delta$.

4.1. Strong decoherence

For strong edge-state decoherence, coherent mixing of the quasiparticle states on the two antidots is suppressed, and the quasiparticle dynamics is described by kinetic equations for the occupation probabilities p_{ij} of the states $|ij\rangle$ (2) localized on the antidots. The probabilities evolve due to incoherent jumps of quasiparticles at the rates Γ_Δ (20) and Γ_l (21) between these states. The stationary quasiparticle current I through the antidots is found in this regime from the balance of the forward/backward transition across any of the three tunnel junctions of the system, e.g., from the transitions between the antidots:

$$I = e\nu[p_{10}\Gamma_\Delta(2\delta) - p_{01}\Gamma_\Delta(-2\delta)]. \quad (27)$$

In general, the quasiparticle current I can be calculated by the direct numerical solution of the kinetic equation.

The results of such solution for the linear conductance $G = dI/dV|_{V=0}$ are shown in Fig. 3 (in all numerical results presented below we take $\nu = 1/3$). Qualitative behavior of the system can be understood by analyzing the limits where the simple analytical expressions for the conductance can be obtained.

The first limit is $\Gamma_\Delta \ll \Gamma_l$, where the antidot-antidot tunneling is the bottleneck for the current flow. In this case, to the zeroth-order approximation in Γ_Δ , the current is vanishing, and one can use in Eq. (27) the equilibrium probabilities $p_{ij} = (1/Z)e^{-\epsilon_{ij}/T}$, $Z = \sum_{ij} e^{-\epsilon_{ij}/T}$, obtaining for the conductance:

$$G = \frac{(e\nu)^2 \gamma}{T} \frac{f_g(2\delta)e^{\delta/2T}}{e^{-\epsilon/T} + e^{-(\epsilon+U)/T} + 2 \cosh(\delta/T)}. \quad (28)$$

Equation (28) describes the “coalesced” conductance peak that corresponds to the addition of two quasiparticles to the antidots. At large temperatures, $T \geq U$, the peak has a usual thermally-broadened shape with width proportional to T . At $T \ll U$, however, the peak shape (28) is quite unusual: the conductance is constant between the point $\epsilon \simeq 0$, when the first quasiparticle is added to the antidots, and the point $\epsilon \simeq -U$ of addition of the second quasiparticle, forming the plateau of width U – see Fig. 3. The conductance plateau remains flat until the temperature is lowered to $T \simeq U/\ln[\Gamma_l(U)/\Gamma_\Delta]$, when the thermal suppression of the antidot-edge tunneling rate makes it comparable to Γ_Δ at the center of the plateau, $\epsilon \simeq -U/2$, despite the fact that the two rates are very different at $\epsilon \simeq 0$. In this temperature range, a dip develops in the center, which separates the plateau into two peaks, one at $\epsilon \simeq 0$ and the other at $\epsilon \simeq -U$, with decreasing temperature (Fig. 3). Each peak corresponds to addition of one quasiparticle to the double-antidot system. Note that the resonant peaks occur when the gate bias energy ϵ is equal to “minus energy” of the antidot state, so that the total energy of the state relative to the chemical potential of the edges is zero.

The shape of such single-quasiparticle peaks can be described in the opposite limit of strong antidot-antidot tunneling $\Gamma_\Delta \gg \Gamma_l$. In this limit, the general kinetic equations for three probabilities p_{00}, p_{10}, p_{01} relevant at $\epsilon \simeq 0$, e.g.,

$$\dot{p}_{00} = \Gamma_1(-\epsilon_1)p_{10} + \Gamma_2(-\epsilon_2)p_{01} - [\Gamma_1(\epsilon_1) + \Gamma_2(\epsilon_2)]p_{00}, \quad (29)$$

and similar equations for the other probabilities, can be reduced to two equations for the effective two-state system. The strong antidot-antidot tunneling that couples the singly-occupied states $|10\rangle, |01\rangle$, maintains the relative equilibrium between them: $p_{10}/p_{01} = e^{-2\delta/T}$, making it possible to treat these two states as one. The effective transition rates between this state and the state $|00\rangle$ are obtained as the weighted average of the transition rates in starting kinetic equations, e.g. (29). The standard calculation of the current through a two-state system gives then the resonant peak of the double-antidot conductance at $\epsilon \simeq 0$ (associated with addition of the first quasiparticle to the antidots):

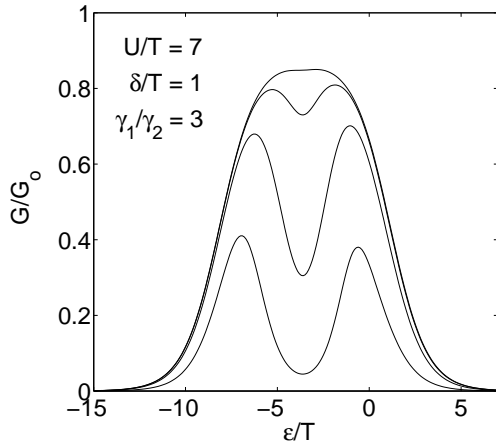


Fig. 3. Conductance of the double-antidot system in the regime of overdamped quasiparticle transport. Conductance is normalized to $G_0 = (e\nu)^2 \Gamma_\Delta(2\delta)/T$. Different curves correspond to different ratios of the antidot-antidot and antidot-edge tunneling rates. From top to bottom: $\Gamma_\Delta(2\delta)/\Gamma_2(0) = 10^{-4}, 10^{-3}, 10^{-2}, 10^{-1}$.

$$G = \frac{(e\nu)^2 \Gamma_1(\epsilon_1) \Gamma_2(-\epsilon_2) f(2\delta)/T}{\Gamma_1(\epsilon_1) + \Gamma_2(\epsilon_2) + \Gamma_1(-\epsilon_1) f(-2\delta) + \Gamma_2(-\epsilon_2) f(2\delta)}, \quad (30)$$

where $f(E) = f_1(E)$ is the Fermi distribution function. For instance, if the two antidot states are aligned, $\delta = 0$,

$$G = \frac{(e\nu)^2}{T} \frac{\gamma_1 \gamma_2}{\gamma_1 + \gamma_2} \frac{f_\nu(\epsilon)}{1 + 2e^{-\epsilon/T}}. \quad (31)$$

The conductance peak at $\epsilon \simeq -U$ associated with the addition of the second quasiparticle is given by an expression similar to Eq. (30) with an appropriate shift of energy $\epsilon \rightarrow \epsilon + U$. In particular, for $\delta = 0$, this expression reduces to

$$G = \frac{(e\nu)^2}{T} \frac{\gamma_1 \gamma_2}{\gamma_1 + \gamma_2} \frac{f_\nu(\epsilon + U)}{2 + e^{-(\epsilon + U)/T}}. \quad (32)$$

The conductance peak (31) is asymmetric around $\epsilon = 0$, since in the tunneling dynamics underlying this peak, only one quasiparticle can tunnel off the antidots, while there are two available states for tunneling onto the antidots. Still, the “quasiparticle-quasihole” symmetry makes the two peaks, (31) and (32), at $\delta = 0$ symmetric images of each other with respect to a “mirror” reflection $\epsilon + U/2 \rightarrow -(\epsilon + U/2)$. For $\delta \neq 0$, the condition $\Gamma_\Delta \gg \Gamma_l$ is violated at sufficiently low temperatures $T \ll \delta$, and Eq. (30) becomes invalid. In this case, the antidots are effectively out of resonance, and conductance peaks are suppressed exponentially with temperature at all gate bias energies ϵ .

4.2. Weak decoherence

If the edge-state decoherence is sufficiently weak and allows for quantum-coherent transfer of quasiparticles between the two antidots, the kinetic equation for quasiparticle transport should be written not in the basis of states, (2), but in the basis of the hybridized states (23). As follows from the estimates of the edge-state decoherence in

Sec. 2.3, even in this regime, the edge-induced relaxation rate Γ_d (14) should be strong enough, $\Gamma_d \gg \Gamma_l$, to maintain the equilibrium distribution of quasiparticles over the antidot states in the process of tunneling. This means that if $E_k^{(n)}$ is the energy of the state $|k\rangle$ when there are n quasiparticles on the antidots, the probability that this state is occupied is $\rho_k(n) = (1/Z_n) e^{-E_k^{(n)}/T}$, $Z_n = \sum_k e^{-E_k^{(n)}/T}$. The quasiparticle tunneling is reduced then to the dynamics of the total number n of quasiparticles on the antidots, described by the probability distribution $p(n)$. The rates of tunneling transitions $n \rightarrow n \pm 1$ in this dynamics are:

$$\Gamma^\pm(n) = \sum_{l=1,2} \Gamma_l^\pm(n), \quad \Gamma_l^\pm(n) = \sum_{kq} \rho_k(n) \Gamma_l(k, q, n, n \pm 1),$$

where the partial transitions rates $\Gamma_l(p, k, n, n \pm 1)$ from the state k of n quasiparticles into the state k' of $n \pm 1$ quasiparticles are given by the appropriate tunneling rates (26) between the l th edge and antidot. The solution of the simple kinetic equation

$$\dot{p}(n) = \sum_{\pm} [\Gamma^\mp(n \pm 1) p(n \pm 1) - \Gamma^\pm(n) p(n)], \quad (33)$$

gives then the stationary quasiparticle current through the system:

$$I = \nu e \sum_n [\Gamma_1^+(n) P(n) - \Gamma_1^-(n-1) P(n-1)]. \quad (34)$$

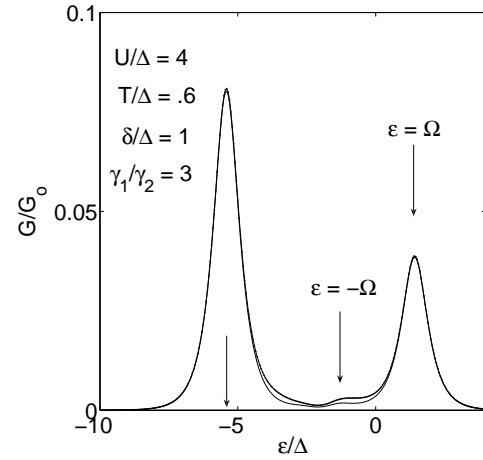


Fig. 4. Conductance of the double-antidot system in the regime of the underdamped quasiparticle dynamics. Conductance is plotted in units of $G_0 = (e\nu)^2 \Gamma_1(0)/T$. The curves show the two main resonant conductance peaks at $\epsilon = \Omega$ and $\epsilon = -(U + \Omega)$, and a weak kink at $\epsilon = -\Omega$ that is made visible by the Luttinger-liquid singularity in the tunneling rates. The upper and lower curves are, respectively, the conductance with and without equilibration on the antidots.

Equation (33) shows that the stationary probability distribution $p(n)$ satisfies the “detailed balance” condition $p(n)\Gamma^+(n) = p(n+1)\Gamma^-(n+1)$ even in the presence of the non-vanishing bias voltage V . Using this condition, and

expanding both $p(n)$ and the tunneling rates $\Gamma(n)$ to first order in V , one finds the linear conductance G of the quasiparticle qubit:

$$G = \eta \frac{(e\nu)^2}{T} \sum_n w_n \frac{\Gamma_1^+(n)\Gamma_2^+(n)}{\Gamma_1^+(n) + \Gamma_2^+(n)}. \quad (35)$$

Here $w_n = Z_n/Z$ is the equilibrium probability to have n quasiparticles on the antidots, $Z = \sum_n Z_n$, and the factor η gives the fraction of the voltage V that drops across the edge-antidot junctions. Equation (35) can be understood in terms of forward jumps of quasiparticles in the left junction contributing to the current only if they are followed by the forward jumps in the right junction. As an example, at temperatures $T \ll U$, and $\epsilon \simeq -\Omega$ one can limit the sum in Eq. (35) to one term $n = 0$. The conductance G is then:

$$G = \frac{(e\nu)^2}{T} \frac{\eta}{1 + 2e^{-\epsilon/T} \cosh(\Omega/T)} \cdot \frac{\sum_{q,k} \Gamma_{1q}(\epsilon + (-1)^q \Omega) \Gamma_{2k}(\epsilon + (-1)^k \Omega)}{\sum_{l,m} \Gamma_{lm}(\epsilon + (-1)^m \Omega)}, \quad (36)$$

where the tunneling rates Γ_{qk} are defined in Eq. (26).

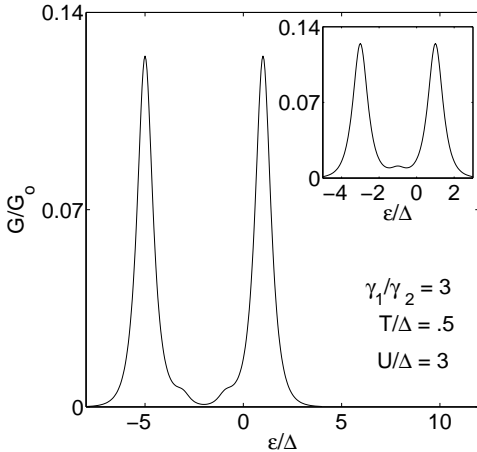


Fig. 5. Conductance of the symmetric ($\delta = 0$) antidot qubit exhibiting two resonant conductance peaks at $\epsilon = \Delta$ and $\epsilon = -(U + \Delta)$. Both peaks have kinks at $\epsilon = -\Delta$ and $\epsilon = -(U - \Delta)$ caused by the Luttinger-liquid singularity in the tunneling rates. The inset shows the conductance for the special value of interaction energy $U = 2\Delta$, when the two kinks coincide producing very small but visible additional conductance peak. Conductance is normalized as in Fig. 4.

For comparison, one can calculate the conductance in the same regime $T \ll U$, $\epsilon \simeq -\Omega$, but without equilibration on the antidots, i.e. assuming that the edge-state decoherence is very weak, $\Gamma_d \ll \Gamma_l$. As before, the antidots can be occupied in this regime at most by one quasiparticle at a time, and straightforward solution of the kinetic equation describing the occupation of individual energy eigenstates due to transitions (26) gives the conductance:

$$G = \frac{(e\nu)^2}{T} \frac{\Delta^2}{2\Omega^2} \frac{\eta\gamma_1\gamma_2}{1 + 2e^{-\epsilon/T} \cosh(\Omega/T)}.$$

$$\sum_{\pm} \frac{f_{\nu}(\epsilon \pm \Omega)}{\gamma_1(1 \mp \delta/\Omega) + \gamma_2(1 \pm \delta/\Omega)}. \quad (37)$$

Equation (37) describes the resonant conductance peak that corresponds to the addition of the first quasiparticle to the antidot. The second quasiparticle peak at $\epsilon = -(U + \Omega)$ is described by the similar expression. At low temperatures, $T \ll \Omega$, only the lowest energy eigenstate with energy $-\Omega$ contributes to the conductance (37). In this case, the equilibration on the antidots does not have any effect, and Eqs. (36) and (37) coincide. As one can see from Fig. 4, which plots the conductance obtained by numerical solution of the full kinetic equation, the difference between the two regimes, with and without relaxation, remains very small even at moderate temperatures. At larger temperatures, $\Omega \ll T \ll U$, and $\delta = 0$, Eq. (37) reduces to Eq. (31) for the conductance in the overdamped regime. The only difference between the two results is the factor η in Eq. (37) which implies that the part of the applied bias voltage that drops across the region of the quantum-coherent quasiparticle dynamics does not contribute to the linear conductance.

Besides the two main resonant peaks, the curves in Fig. 4 exhibit also a small kink at $\epsilon \simeq -\Omega$. This kink appears at the intermediate temperatures and is the result of the transfer of the first quasiparticle added to the antidots not through the more probable ground state of the qubit but through the excited state with energy Ω . One could see, however, by plotting the conductance of the double-antidot system for tunneling electrons (the tunneling rates given by the $g = 1$ in Fig. 2) that the contribution of the excited state to the conductance is not sufficient by itself to produce such a kink. The kink in the conductance appears only when the contribution from the excited state is amplified by the Luttinger-liquid singularity in the quasiparticle tunneling rate (seen in the $g = 1/3$ curve in Fig. 2 as a peak at zero energy). It becomes somewhat more pronounced in the conductance peaks of the “symmetric” qubit with $\delta = 0$ shown in Fig. 5. In this case, the kinks appear on both peaks: at $\epsilon = -\Delta$ and $\epsilon = -(U - \Delta)$. The second kink is due to transport through the ground state of the qubit in the regime when the main contribution to conductance comes from the excited state. As shown in the inset in Fig. 5, at the special value of the interaction energy $U \simeq 2\Delta$, the two kinks coincide and form a weak additional peak of the qubit conductance.

5. Conclusion

We have calculated the linear conductance G of the double-antidot system in the regime of weak quasiparticle tunneling through the antidots. Depending on the strength of the edge-state decoherence, the tunneling can be coherent or incoherent. In the incoherent regime, the two resonant conductance peaks that correspond to the two antidot states are spaced by the quasiparticle interaction energy U . In the coherent regime, this spacing is

increased to $U + 2\Omega$, where 2Ω is the gap between the energy eigenstates of the double-antidot system. The coherent regime of quasiparticle dynamics is also characterized by the Lorentzian dependence of the system conductance, $G \propto (1 + \delta^2/\Delta^2)^{-1}$, on the energy difference δ between the antidots. In the quantum-coherent regime, the double-antidot system can be used as a quasiparticle qubit.

The authors would like to thank V.J. Goldman for many useful discussions of the antidot transport. This work was supported in part by NSF grant # DMR-0325551 and by ARO grant # DAAD19-03-1-0126.

- [24] K.T. Law, D.E. Feldman, and Y. Gefen, Phys. Rev. B **74**, 045319 (2006).
- [25] D.V. Averin and A.N. Korotkov, Sov. Phys. JETP **70**, 937 (1990); C.W.J. Beenakker, Phys. Rev. B **44**, 1646 (1991); D.V. Averin, A.N. Korotkov, and K.K. Likharev, Phys. Rev. B **44**, 6199 (1991).
- [26] C. de C. Chamon and X.G. Wen, Phys. Rev. Lett. **70**, 2605 (1993).
- [27] A. Furusaki and N. Nagaosa, Phys. Rev. B **47**, 3827 (1993).
- [28] X.G. Wen, Phys. Rev. B **44**, 5708 (1991); Y. Oreg and A.M. Finkel'stein, Phys. Rev. Lett. **74**, 3668 (1995); V.J. Goldman and E.V. Tsiper, Phys. Rev. Lett. **86**, 5841 (2001).

References

- [1] R.B. Laughlin, Phys. Rev. Lett. **50**, 1395 (1983); Rev. Mod. Phys. **71**, 863 (1999).
- [2] B.I. Halperin, Phys. Rev. Lett. **52**, 1583 (1984).
- [3] D. Arovas, J.R. Schrieffer, and F. Wilczek, Phys. Rev. Lett. **53**, 722 (1984).
- [4] V.J. Goldman and B. Su, Science **267**, 1010 (1995); V.J. Goldman, I. Karakurt, J. Liu, and A. Zaslavsky, Phys. Rev. B **64**, 085319 (2001).
- [5] I.J. Maasilta and V.J. Goldman, Phys. Rev. B **57**, R4273 (1998).
- [6] M. Kataoka, C.J.B. Ford, G. Faini, D. Mailly, M.Y. Simmons, D.R. Mace, C.-T. Liang, and D.A. Ritchie, Phys. Rev. Lett. **83**, 160 (1999).
- [7] L. Saminadayar, D.C. Glattli, Y. Jin, and B. Etienne, Phys. Rev. Lett. **79**, 2526 (1997).
- [8] R. de-Picciotto, M. Reznikov, M. Heiblum, V. Umansky, G. Bunin, D. Mahalu, Nature **389**, 162 (1997); M. Reznikov, R. de Picciotto, T.G. Griffiths, M. Heiblum, and V. Umansky, Nature **399**, 238 (1999).
- [9] D.V. Averin and K.K. Likharev, in: "Mesoscopic Phenomena in Solids" (eds. B.L. Altshuler, P.A. Lee, and R.B. Webb) p. 173 (Elsevier, Amsterdam, 1991).
- [10] L.P. Kouwenhoven, C.M. Marcus, P.L. McEuen, S. Tarucha, R.M. Westervelt, and N.S. Wingreen, in: "Mesoscopic Electron Transport" (eds. L.L. Sohn, L.P. Kouwenhoven, and G. Schön) p. 105 (Kluwer, Dordrecht, 1997).
- [11] M.R. Geller, D. Loss, and G. Kirczenow, Phys. Rev. Lett. **77**, 5110 (1996).
- [12] D.V. Averin and V.J. Goldman, Solid State Commun. **121**, 25 (2002).
- [13] D.V. Averin, Solid State Commun. **105**, 659 (1998).
- [14] A. Shnirman, G. Schön, and Z. Hermon, Phys. Rev. Lett. **79**, 2371 (1997); Yu. Makhlin, G. Schön, and A. Shnirman, Nature **398**, 305 (1999).
- [15] D.J. Flees, S. Han, and J. E. Lukens, Phys. Rev. Lett. **78**, 4817 (1997).
- [16] Y. Nakamura, C.D. Chen, and J.S. Tsai, Phys. Rev. Lett. **79**, 2328 (1997).
- [17] S. Das Sarma, M. Freedman, and C. Nayak, Phys. Rev. Lett. **94**, 166802 (2005).
- [18] L.S. Georgiev, Phys. Rev. B **74**, 235112 (2006).
- [19] X.G. Wen, Adv. Phys. **44**, 405 (1995).
- [20] V.V. Ponomarenko and D.V. Averin, JETP Lett. **74**, 87 (2001); Phys. Rev. B **70**, 195316 (2004).
- [21] I. Safi, P. Devillard, and T. Martin, Phys. Rev. Lett. **86**, 4628 (2001).
- [22] C.L. Kane, Phys. Rev. Lett. **90**, 226802 (2003).
- [23] V.V. Ponomarenko and D.V. Averin, Phys. Rev. B **71**, 241308(R) (2005).